Title

Recent Results Using Synchrotron Radiation for Energy Dispersive X-Ray Fluorescence Analysis

Authors

Jaklevic, J M
Giauque, R D
Thompson, A C

Publication Date

1989-04-01

LBL-27135
Preprint

Lawrence Berkeley Laboratory
UNIVERSITY OF CALIFORNIA

Engineering Division

Submitted to X-Ray Spectrometry

Recent Results Using Synchrotron Radiation for Energy Dispersive X-Ray Fluorescence Analysis

J.M. Jaklevic, R.D. Giauque, and A.C. Thompson

April 1989

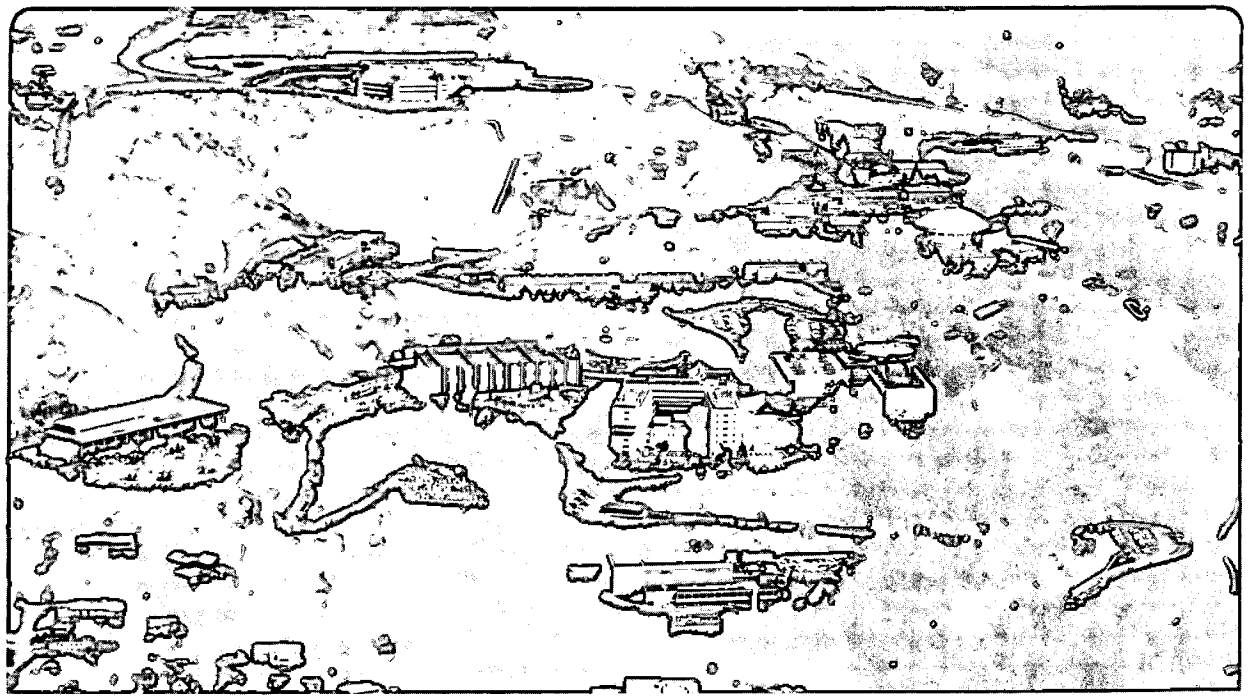

Prepared for the U.S. Department of Energy under Contract Number DE-AC03-76SF00098.

DISCLAIMER

J. M. Jaklevic,
R. D. Giauque
and A. C. Thompson

Engineering Division
Lawrence Berkeley Laboratory
One Cyclotron Road
Berkeley, California 94720 U.S.A.

RECENT RESULTS USING SYNCHROTRON RADIATION FOR ENERGY DISPERSIVE X-RAY FLUORESCENCE ANALYSIS

Abstract

Results obtained using synchrotron radiation as an excitation source for energy dispersive analysis are reviewed. Practical experience gained in the use of tunable, monochromatic excitation for trace analysis of various types of samples is discussed. Advantages and limitations associated with specific synchrotron radiation properties will be evaluated. In particular, the influence of multiple inelastic scattering and resonant Raman scattering on limiting the degree of detectability improvements associated with energy tuning is demonstrated. A scanning x-ray microprobe employing multilayer mirrors as focusing elements is described. Measurements performed with this system have demonstrated the capability of detecting femtogram quantities of trace elements in a 10 μm x 10 μm area.

Introduction

Synchrotron sources are capable of generating intense, highly collimated beams of linearly polarized electromagnetic radiation with continuum energy distributions which overlap the region of interest for elemental analysis using x-ray fluorescence. Modern source designs which incorporate magnetic insertion devices can provide enhanced intensity and brightness over an energy range extending from below 1 keV to greater than 20 keV. Information regarding the properties of such sources is available in a number of review publications.[1-3]

Several recent studies have explored the properties of synchrotron radiation as an excitation source for energy dispersive x-ray fluorescence analysis.[4-12, 19] Experiments have demonstrated several advantages in the use of synchrotron radiation relative to more conventional approaches to energy dispersive x-ray fluorescence analysis. The principal advantage arises from the dramatic increase in available excitation flux. Table 1 compares the intensity of radioisotope sources and conventional x-ray tubes to typical state-of-the-art synchrotron sources. It is important to emphasize that the synchrotron radiation is both highly collimated and continuous in energy so that the intensity quoted for a 1 eV bandpass represents only a small fraction of the total continuum flux available. More complete descriptions of synchrotron radiation properties for various types of sources are contained in Refs. 1-3. In addition to providing a significant increase in usable output flux, there are other unique properties of synchrotron radiation which can be exploited to provide enhanced capabilities for many energy dispersive x-ray fluorescence analysis applications.

For example, the ability to continuously select the excitation energy by means of a crystal monochromator provides one with a capability for optimizing the analytical sensitivity for a particular range of elements and discriminate against others. The polarization of the incident radiation can be used to reduce the relative contribution of scattered radiation reaching the detector. Finally, the high degree of collimation inherent in the beam profile facilitates the application of x-ray optical methods for focusing the radiation to microscopic dimensions.

In the following discussion, we summarize results obtained in a series of studies designed to explore the application of synchrotron radiation to the analysis of a wide class of samples with particular emphasis on trace element studies. Specific issues which have been investigated include the advantages of tunable monochromatic excitation, methods for reduction of scattered background, and the design of microfocused beams using x-ray focusing elements. It has been found that, although significant improvements can be achieved by using synchrotron radiation excitation, there are still fundamental limitations which limit the degree of improvement.

Experimental Procedures

A schematic illustration of a typical energy dispersive x-ray fluorescence analysis geometry using synchrotron radiation excitation is seen in Fig. 1. The collimated source from the accelerator is incident from the right in the example shown. A double crystal monochromator can be inserted in the beam path for energy tuning. The beam profile is defined by slit or aperture collimators placed before the sample. Ionization chambers are used to monitor the intensity of the incident and, in some cases, the transmitted beam. Comparison of data from one run to the next is achieved by normalization of the spectra to an equivalent amount of incident flux on the first ionization chamber. A suitably shielded energy dispersive semiconductor detector spectrometer views the sample at an angle of 90° with respect to the incident beam. The sample is inserted in the beam path using a scanning stage to provide remote manipulation of the sample(s) within the radiation safety enclosure.

Monochromatic Energy Tuning

The potential advantages of tuning the energy of the source result from the strong energy dependence of the inner shell photoelectric cross section. For incident photon energies directly above a major absorption edge, the cross section is a maximum and decreases proportional to $(E)^{-3}$ as the energy increases. Optimal excitation efficiency for a given element is then achieved using excitation energies directly above the absorption edge corresponding to the particular emission line being measured. Discrimination against major matrix elements of atomic number higher than the element of interest in the sample can also be realized by tuning the excitation below the edge of the major element.

Although the maximum excitation efficiency for a particular element occurs at the absorption edge energy, the excitation energy for optimum analytical sensitivity is slightly different. Figure 2 illustrates the effect of energy tuning on the experimentally measured minimum detectable limits (3 σ) of the four elements Mn, Zn, Se and Rb for the case of a hydrocarbon matrix.[12] The qualitative behavior which one might predict is illustrated for the case of Mn where the detectable limit improves as the excitation energy is reduced from 20 to 8 keV. Unfortunately, the improvement does not continue as the K-absorption edge is approached. In spite of the maximum cross section for fluorescence excitation for energies directly above the absorption edge, improvement in analytical sensitivity is mitigated by an increase in interfering background due to multiple scattering of the incident photons from the sample matrix. This is illustrated in Fig. 3 which shows a spectrum obtained by scattering 17 keV radiation from a 30 mg/cm^2 cellulose pellet.[11] Several unresolved peaks due to multiple, incoherent scattering events extend the background level to lower energies than that anticipated from a single, 90° scattering event.

Discrimination against overlapping x-ray emission lines can be achieved in favorable cases by tuning the excitation energy below the major absorption edge of the interfering element. Figure 4 illustrates an example in which the well known case of Pb L-α/ As K-α interference is successfully

addressed.[11] The sample is a fine-particle urban atmospheric aerosol sample in which lead is present at a concentration of 460 ng/cm^2. By tuning the excitation energy to 12.9 keV, the Pb L-α line is no longer excited and the As K-α emission line corresponding to 2 ng/cm^2 is observed.

However, the ability to discriminate against major matrix elements by tuning below the edge has been found to be limited by the presence of scattering effects not normally considered in energy dispersive x-ray fluorescence.[13] Figure 5 illustrates the scattered background measured for a single crystal GaAs semiconductor sample. As the energy is varied below the Ga and As K-absorption edges, a background component attributed to resonant x-ray Raman scattering is seen to interfere with the sensitive detection of low energy x-rays. This scattering is a second order process in which the incident photon is inelastically scattered from the target atoms. The incident photon experiences a discrete energy loss governed by the availability of internal excitations in the target atoms. Although normally a weak effect compared to the Rayleigh and Compton scattering components usually considered in background analysis, the Raman process is resonantly enhanced for incident energies near a major absorption edge. The strong dependence of the scattered intensity in the spectra in Fig. 5 reflects this resonant behavior. It has been estimated that the presence of this anomalous scattering effect causes a reduction of minimum detectability by an order of magnitude or more. For measurements involving samples with significant proportions of heavier elements (i.e., Z>20), the potential effect of resonant Raman scattering must be considered.

Polarization Effects on Background

The background below fluorescent peaks in a photon-excited energy dispersive spectrum is normally directly proportional to the intensity of the major scattered peaks which occur at energies at or near the incident photon energy. This imposes a limit on the sensitivity with which

fluorescent x-rays can be measured, particularly for the case of trace element studies in which the predominant mode of interaction of the incident x-rays involves scattering from the matrix atoms. Figure 3 is an extreme example of this in which the sample consists of a hydrocarbon matrix replicated by a cellulose pellet. Detection of fluorescence x-rays at energies even well below this main scattering distribution is hindered by a continuum background caused by incomplete charge collection of events in the full energy peak.[14] Improvement in analytical detectability can be achieved by reducing this unwanted background either by improving the charge collection in the detector or by reducing the magnitude of the scattered intensity relative to the fluorescent signal.

Modern energy dispersive x-ray spectrometers have been designed to reduce the effects of incomplete charge collection in the detector to a minimum using either internal or external collimation. Synchrotron radiation polarization provides a means of reducing the intensity of the scattered background detected at specific angles.

The dominant effects which contribute to the background intensity in typical x-ray fluorescence measurements are coherent Rayleigh scattering and incoherent Compton scattering. For linearly polarized radiation, both processes exhibit minima in the differential cross sections for angles near 90° with respect to the polarization direction although the angular distributions of the two scattering mechanisms is slightly different. The differential cross-section for Rayleigh scattering is described by a modification of Thomson scattering[15]:

$$\left(\frac{d\sigma}{d\Omega}\right)_R = r_o^2 f^2(q,Z) \cos^2 \propto \qquad (1)$$

whereas Compton scattering is described by the Klein-Nishina formula:

$$\left(\frac{d\sigma}{d\Omega}\right)_c = \frac{r_o^2}{4} S(q,Z) \left(\frac{K}{K_o}\right)^2 \left(\frac{K}{K_o} + \frac{K_o}{K} + 4 \cos^2 \propto - 2\right) \qquad (2)$$

where: r_o^2 = classical electron radius

f(q,Z) = atomic form factor

S(q,Z) = incoherent scattering factor

q = momentum transfer

α = angle between the incident and scattered electric field vectors

$\left(K/K_o\right)$ = ratio of scattered to incident energies

The angular dependence of these two expressions are equivalent in the low-energy limit where the Compton scattered energy is equal to the incident energy. For many synchrotron x-ray fluorescence applications this approximation is valid. (For example, at 20 keV incident energy, the 90° Compton scattered photon has an energy of 19.25 keV.) Hanson has shown that in this limiting case, either expression reduces to the form:

$$\frac{d\sigma}{d\Omega} \propto 1 - \sin^2\theta \cos^2\phi \qquad (3)$$

where θ is the angle between incident and scattered x-ray in the plane of polarization of the incident beam and ϕ is the angle in a plane perpendicular to this. For purposes of semi-quantitative analysis, this can be further simplified by combining the two angles into a total angle with respect to the original polarization axis. The equation then becomes:

$$\frac{d\sigma}{\alpha\Omega} \propto \sin^2\psi \qquad (4)$$

where ψ is the scattering angle defined with respect to an original polarization axis at 90° relative to the incident beam.

This approximate equation clearly illustrates the potential for reduction in scattered background which can be achieved by performing measurements at an angle of 90° with respect to the incident beam in the plane of the synchrotron orbit, i.e., in the original polarization direction. The scattered radiation is reduced according to Eqn (4) whereas the isotropic fluorescence is maintained.

These effects can be seen graphically in Fig. 6 in which the normalized relative intensities of scattering $\varepsilon_2(\theta)$ and fluorescence $\varepsilon_1(\theta)$ are plotted as a function of the solid angle subtended by the detector at the sample. The abscissa is the ratio of the diameter of a circular detector, r, to the target/detector distance, d. The ratio of scattered to fluorescent intensity is seen to decrease as the solid angle is decreased--for small solid angles this ratio is proportional to $(r/d)^2$. This illustrates the advantages to be obtained by operating at a 90° detector angle and with a minimum possible solid angle consistent with adequate counting rate. In practice, there are additional considerations such as incomplete polarization of the incident beam which reduce the improvements relative to this idealized behavior. For a more complete discussion of polarization effects, the reader is referred to the series of papers by Hanson.[15-17]

The improvements in minimum detectable limits which can be achieved by exploiting the polarization advantages and intensity of synchrotron radiation have been investigated by several authors. Table 2 presents results obtained for both continuum excitation and 10 keV monochromatic excitation for a number of elements in hydrocarbon matrices. Also included are results typically achieved for laboratory sources using equivalent samples. These data are adapted from Ref. 9 and are consistent with similar determinations such as those summarized in Fig. 3 and reported in Ref. 6. Precision and accuracy of synchrotron-induced x-ray fluorescence analysis can be made equivalent to that achieved with laboratory instruments provided provisions are made to correct for variations in the incident flux and for dead time effects resulting from high counting

rates. Giauque, et al.[12] have reported on the analysis of several multielement standards in which agreement with reference values was achieved.

Additional reduction in scattered background and corresponding improvement in minimum detectable limits can also be realized for specific types of samples by exploiting the high degree of collimation inherent with the synchrotron source. Iida, et al.[18] have used a method in which the sample substrate consists of a material capable of reflecting the incident x-rays for very low angles of incidence. The coherent and incoherent scattering contributions arising from the substrate are virtually eliminated and the only background arises from interactions in the sample itself. Using this approach, an absolute minimum detectable limit of 1 pg absolute mass has been achieved for monochromatic excitation.

X-Ray Microprobe Beams

An interesting approach to x-ray analysis which combines many of the advantages of synchrotron sources is the use of small diameter, high intensity beams to perform sensitive trace analysis of very small volumes. Such x-ray microprobes can be achieved using either direct collimation of intense focused beams or by demagnification of a beam spot using x-ray optical elements.[19] The ability to select the energy and exploit the polarization advantages can be maintained.

A particular system which achieves these objectives is shown in Fig. 7. The x-ray microprobe consists of a pair of concave spherical mirrors in a Kirkpatrick-Baez focusing geometry.[20] The mirror surfaces are coated with tungsten/carbon multilayers with 2d spacings selected to provide a high degree of reflectivity and energy selection at 10 keV. The advantages of the multilayers arise partially from the wider bandpass compared to single-crystal Bragg reflectors. This is a useful advantage for microprobe x-ray fluorescence where the energy resolution of the incident beam is of

lesser importance than maximum incident flux. The system shown provides a beam spot of 10 μm x 10 μm with a bandpass of 1 keV at 10 keV average energy. When operated at the X-26C microprobe beam line at the Brookhaven National Synchrotron Light Source (NSLS), a maximum flux of 3 x 10^9 photons/sec was measured within the 100 μm^2 focused spot. Microprobe images of thin samples are acquired by mechanically scanning the sample in a raster pattern while synchronously recording the intensity of the fluorescent x-rays.

Figure 8 shows a series of elemental spectra obtained in a line scan of a "fox" mark on an old paper.[21] Each spectra was acquired for 30 sec and the sample was moved 5 μm between each spectra. The spot is less than 50 μm across and the iron concentration at the peak is 130 $\mu g/cm^2$. Estimates of minimum detectable limits which can be achieved with such a system were obtained from measurements of the background scattered from a thin polypropylene film. These results indicate a minimum detectable limit of 3 fg for selected elements.

Summary

Synchrotron radiation has been shown by several authors to be a powerful tool for energy dispersive x-ray fluorescence analysis. The well-defined properties of synchrotron sources provide the experimenter with unique opportunities for optimizing the excitation conditions for specific applications. As more synchrotron sources become available worldwide, the number of facilities dedicated to performing synchrotron-induced energy dispersive x-ray fluorescence will increase. Combining the synchrotron-excited energy dispersive analysis with microbeam x-ray optical focusing elements has made possible the realization of practical x-ray microprobe analysis systems.

Acknowledgements

This work was supported by the Director's Office of Energy Research, Office of Health and Environmental Research, U.S. Department of Energy under Contract No. DE-AC03-76SF00098.

References

1. H. Winick, in H. Winick and S. Doniach (Eds.), *Synchrotron Radiation Research*, Plenum Press, New York, 1980.

2. G.N. Kulipanov, *Nucl. Instrum. Methods Phys. Res.* **A261**, 1 (1987).

3. H. Winick, *Nucl. Instrum. Methods Phys. Res.* **A261**, 9 (1987).

4. C.J. Sparks, Jr., in H. Winick and S. Doniach (Eds.), *Synchrotron Radiation Research*, Plenum Press, New York, NY, 1980, Chapter 14.

5. A. Knoechel, W. Peterson and G. Tolkiehn, *Nucl. Instrum. Methods Phys. Res.* **208**, 659 (1983).

6. J.V. Gilfrich, E.F. Skelton, S.B. Qadri, J.P. Kirkland and D.J. Nagel, *Anal. Chem.* **55**, 232 (1983).

7. K.W. Jones, B.M. Gordon, A.L. Hanson, J.B. Hastings, M.R. Howells, H.W. Kraner and J.R. Chen, *Nucl. Instrum. Methods Phys. Res.* **B3**, 225 (1984).

8. A.J.J. Bos, R.D. Vis, H. Verhuel, M. Prins, S.T. Davies, D.K. Bowen, J. Makijanic and V. Valkovic, *Nucl. Instrum. Methods B3*, **231**, 232 (1984).

9. A. Iida, K. Sakurai, T. Matsushita and Y. Gohshi, *Nucl. Instrum. Methods Phys. Res.* **228**, 556 (1985).

10. A. Iida, T. Matsushita and Y. Gohshi, *Nucl. Instrum. Methods Phys. Res.* **A235**, 597 (1985).

11. J.M. Jaklevic, R.D. Giauque and A.C. Thompson, *Nucl. Instrum. Methods Phys. Res.* **B10/11**, 303 (1985).

12. R.D. Giauque, J.M. Jaklevic and A.C. Thompson, *Anal. Chem.* **54**, 940 (1986).

13. J.M. Jaklevic, R.D. Giauque and A.C. Thompson, *Anal. Chem.* **60**, 482 (1988).

14. F.S. Goulding and J.M. Jaklevic, *Nucl. Instrum. Methods Phys. Res.* **142**, 323 (1977).

15. A.L. Hanson, *Nucl. Instrum. Methods Phys. Res.* **A243**, 583 (1986).

16. A.L. Hanson, *Nucl. Instrum. Methods Phys. Res.* **A249**, 515 (1986).

17. A.L. Hanson, *Nucl. Instrum. Methods Phys. Res.* **A249**, 522 (1986).

18. A. Iida, A. Yoshinaga, K. Sakurai and Y. Gohshi, *Anal. Chem.* **58**, 394 (1986).

19. K.W. Jones and B.M. Gordon, *Anal. Chem.* **61**, 341A (1989).

20. J.H. Underwood, A.C. Thompson, Y. Wu and R.D. Giauque, *Nucl. Instrum. Methods Phys. Res.* **A266**, 296 (1988).

21. A.C. Thompson, J.H. Underwood, Y. Wu , R.D. Giauque, M.L. Rivers and R. Futernick, "X-ray Microprobe Studies Using Multilayer Focussing Optics," Proceedings of 37th Annual Conference on Applications of X-ray Analysis, to be published in *Advances in X-ray Analysis* **32** (1988).

TABLE 1. Comparison of X-Ray Sources

Radioisotope Sources		
10 mCi		3.7×10^7 photons/sec/steradian*
100 mCi		3.7×10^8 "
X-Ray Tubes (8 keV Characteristic X-rays)		
Low Power (100 watts) air cooled		
2 mA @ 50 kV = 6×10^{18} e^-/sec	$\Rightarrow$	~ 10^{14} photons/sec/steradian*
High Power (1000 watts), water cooled		
20 mA @ 50 kV	$\Rightarrow$	~ 10^{15} "
Rotating Anode (10,000 watts)		
200 mA @ 50 kV	$\Rightarrow$	~ 10^{16} "
Synchrotrons (8 keV Monochromatic X-rays)		
Bending Magnet		~ 10^{13} photons/sec/mrad/eV**
Insertion Device		~10^{15} "

*Typical source-sample geometries reduce the usable flux by two to three orders of magnitude relative to these numbers.

**This represents typical flux for a 1 cm wide beam at 10 m distance from the source.

TABLE 2. Minimum Detectable Limits*

	Synchrotron Excitation (100 sec)			Conventional (600 sec)
Element	Continuum	Continuum with Absorber	Monochromatic (11 keV)	Monochromatic (9.9 keV)
Zn	550 ppb	170 ppb	60 ppb	1900 ppb
Mn	410 ppb	240 ppb	70 ppb	2000 ppb
Ca	440 ppb	750 ppb	200 ppb	8800 ppb

* Adapted from Ref. 9. Data were acquired at a storage ring energy of 2.5 GeV with beam currents between 50 mA and 150 mA.

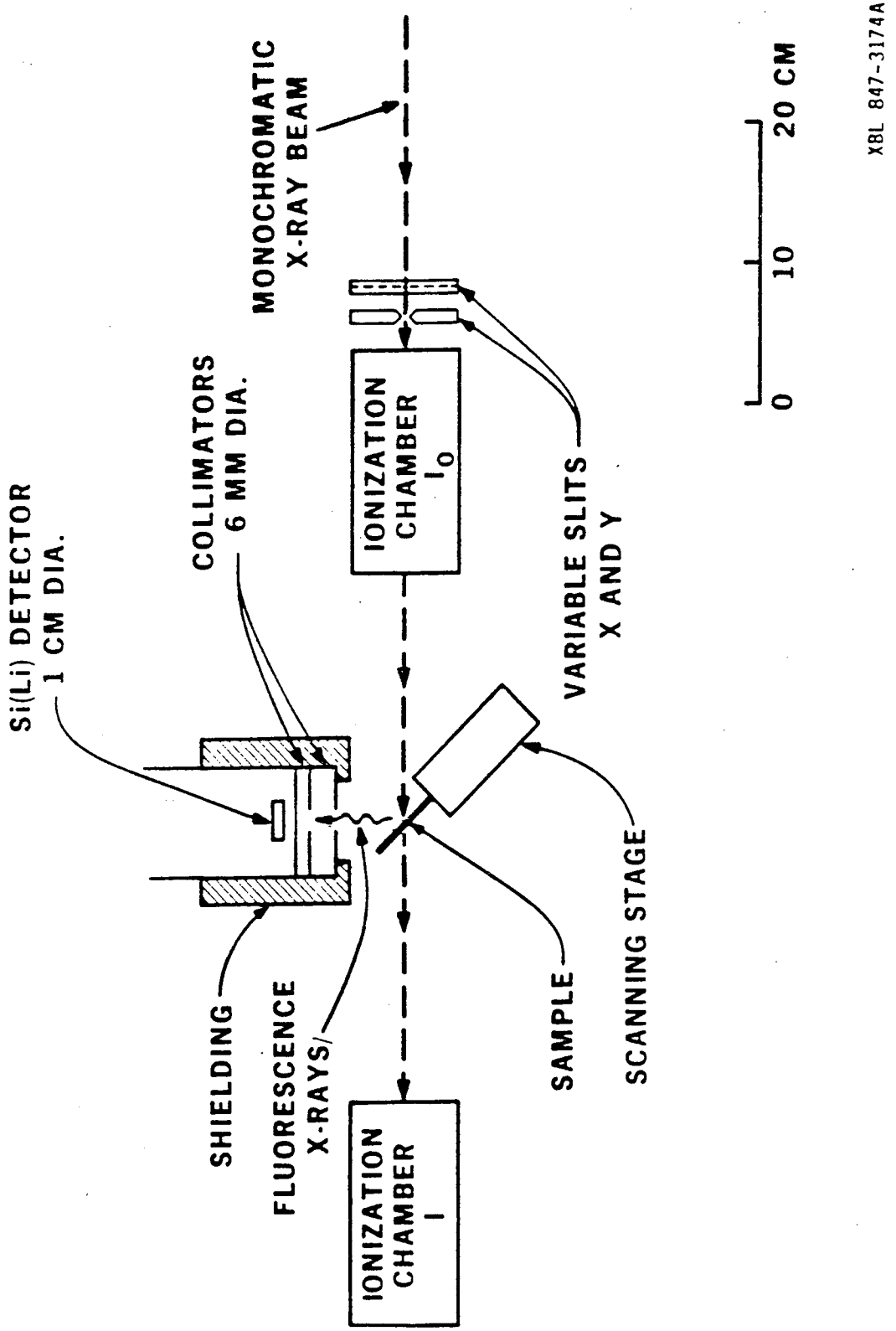

FIG. 1. Schematic diagram of energy dispersive analysis system for synchrotron excitation. The example illustrates the case of monochromatic excitation incident on the sample.

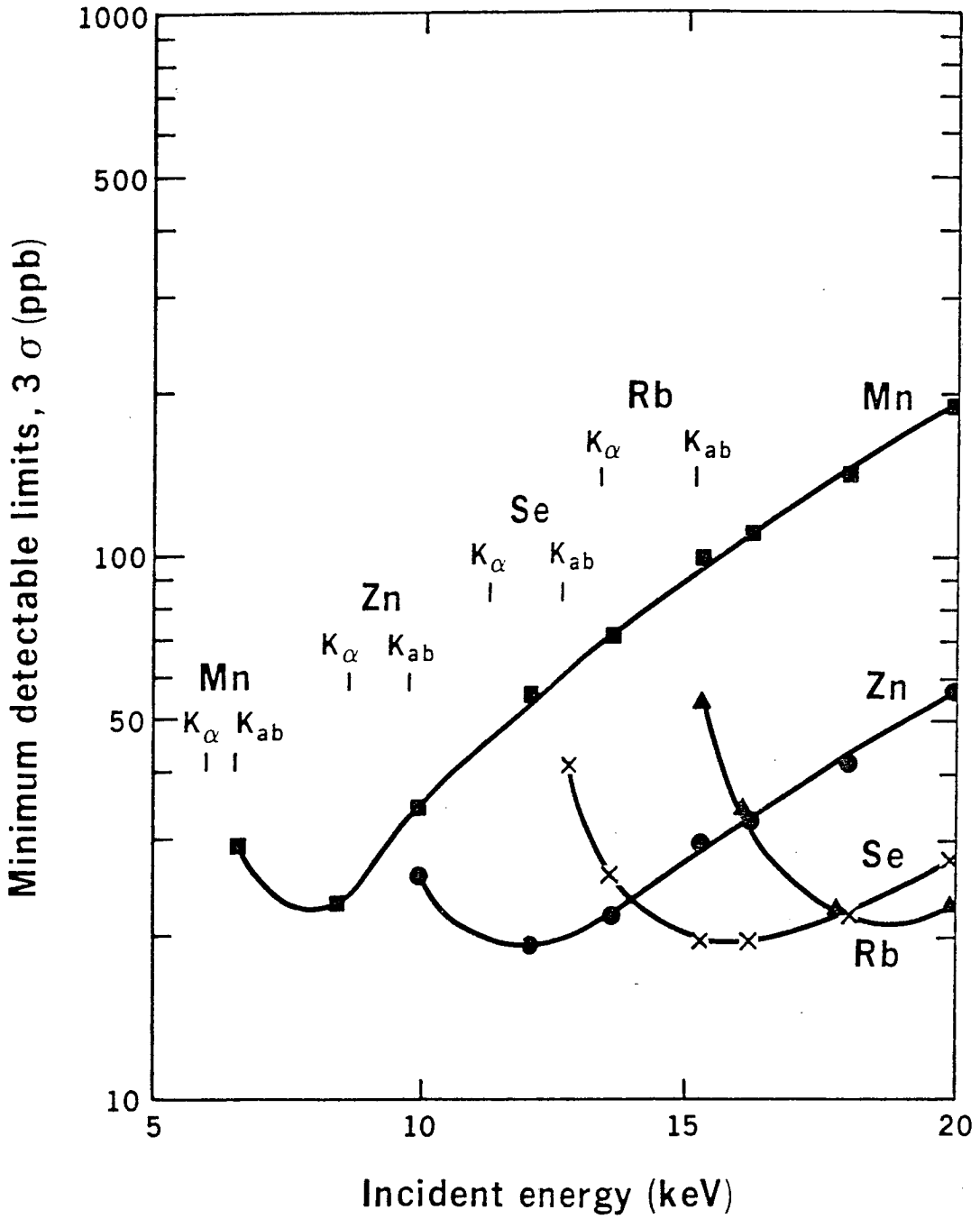

FIG. 2. Minimum detectable limits measured as a function of energy for selected elements. The background was acquired with a 40 mg/cm^2 cellulose disk. Calculations are based on a 300 sec counting interval.

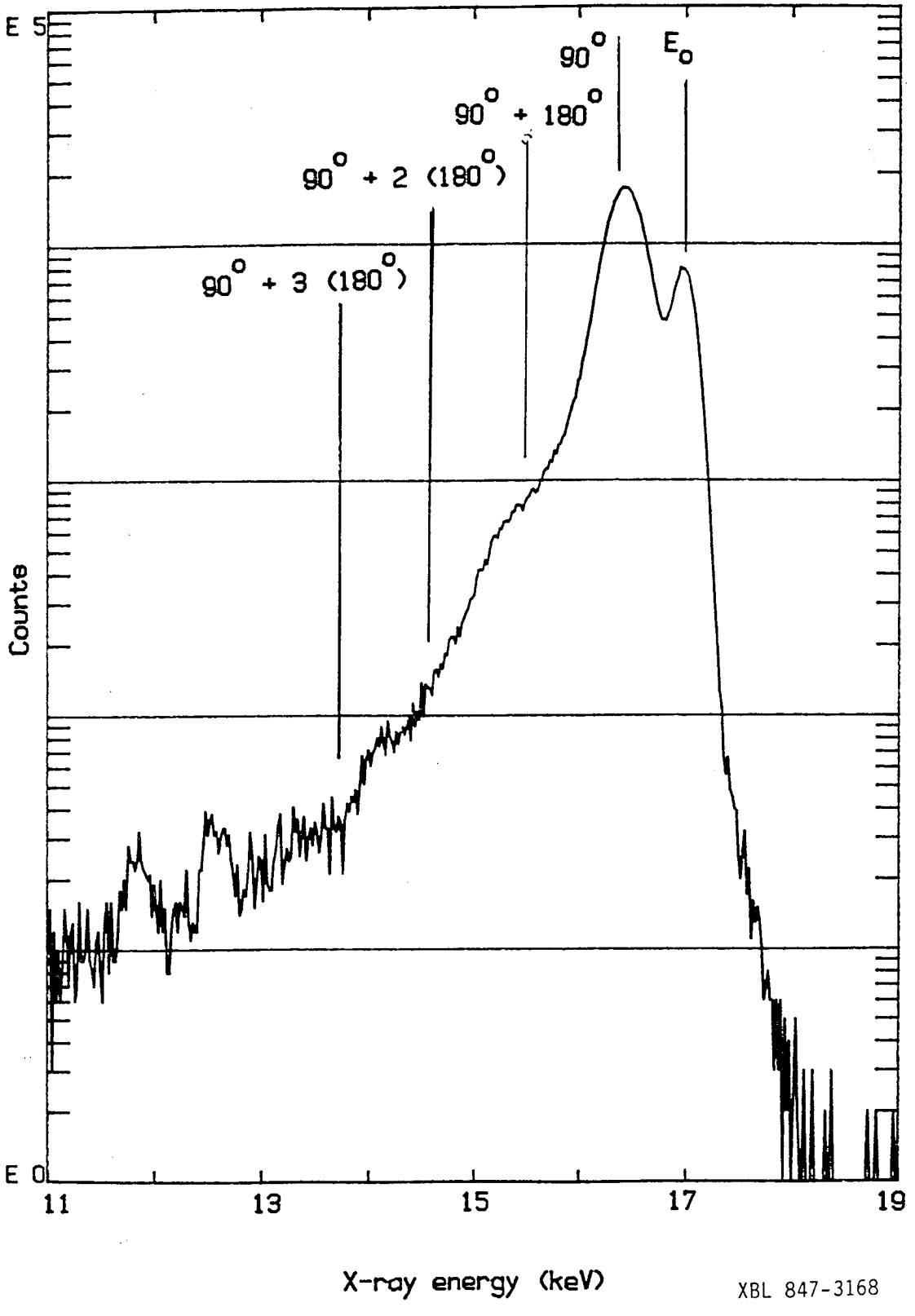

FIG. 3. Background spectrum acquired with a cellulose sample showing multiple incoherent scattering peaks.

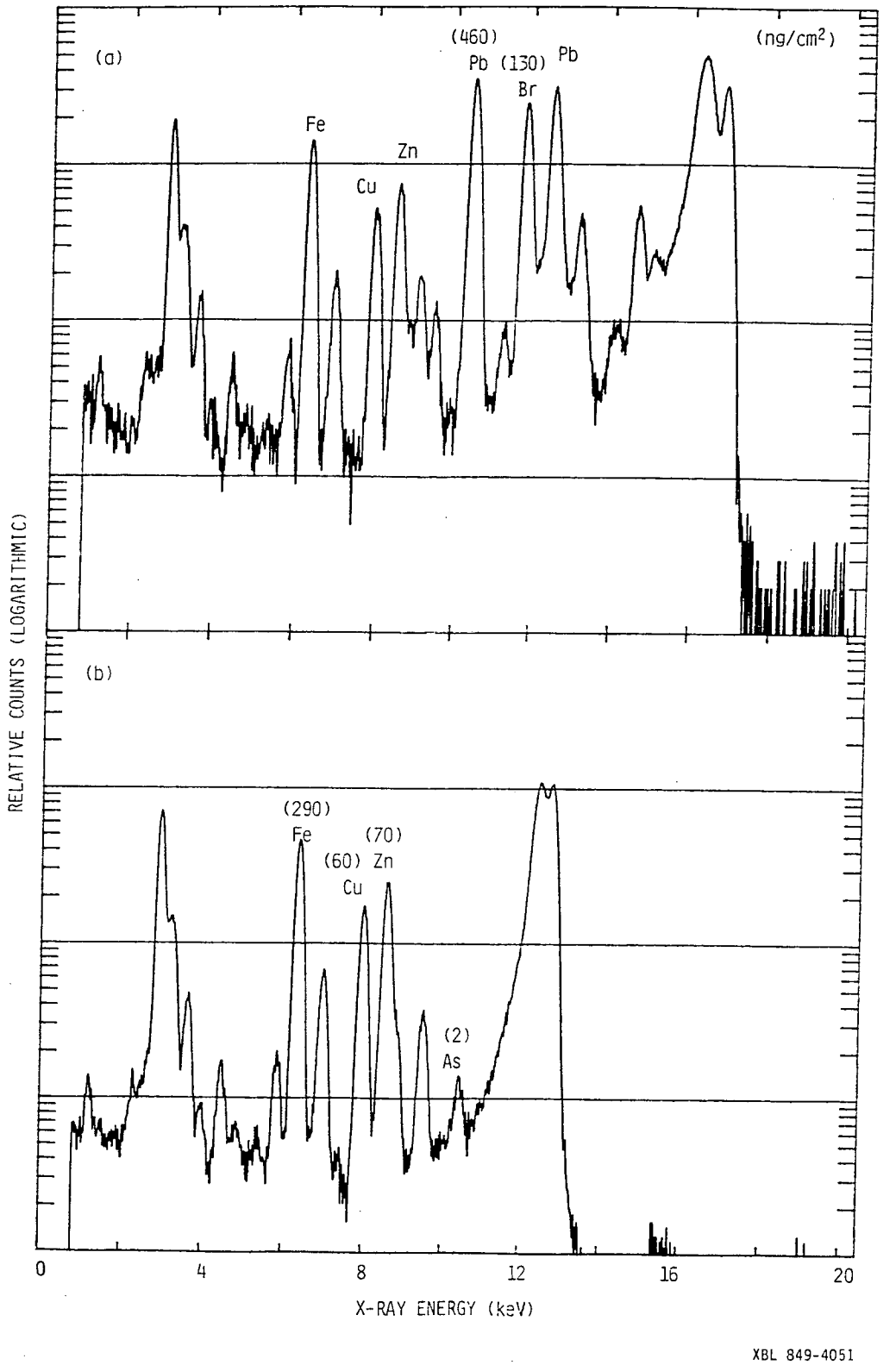

FIG. 4. Spectra of atmospheric aerosol sample acquired at two excitation energies and illustrating the detection of 2 ng/cm^2 As in the presence of 469 ng/cm2 Pb. Spectrum a) was taken with 17.0 keV excitation, spectrum b) at 12.9 keV.

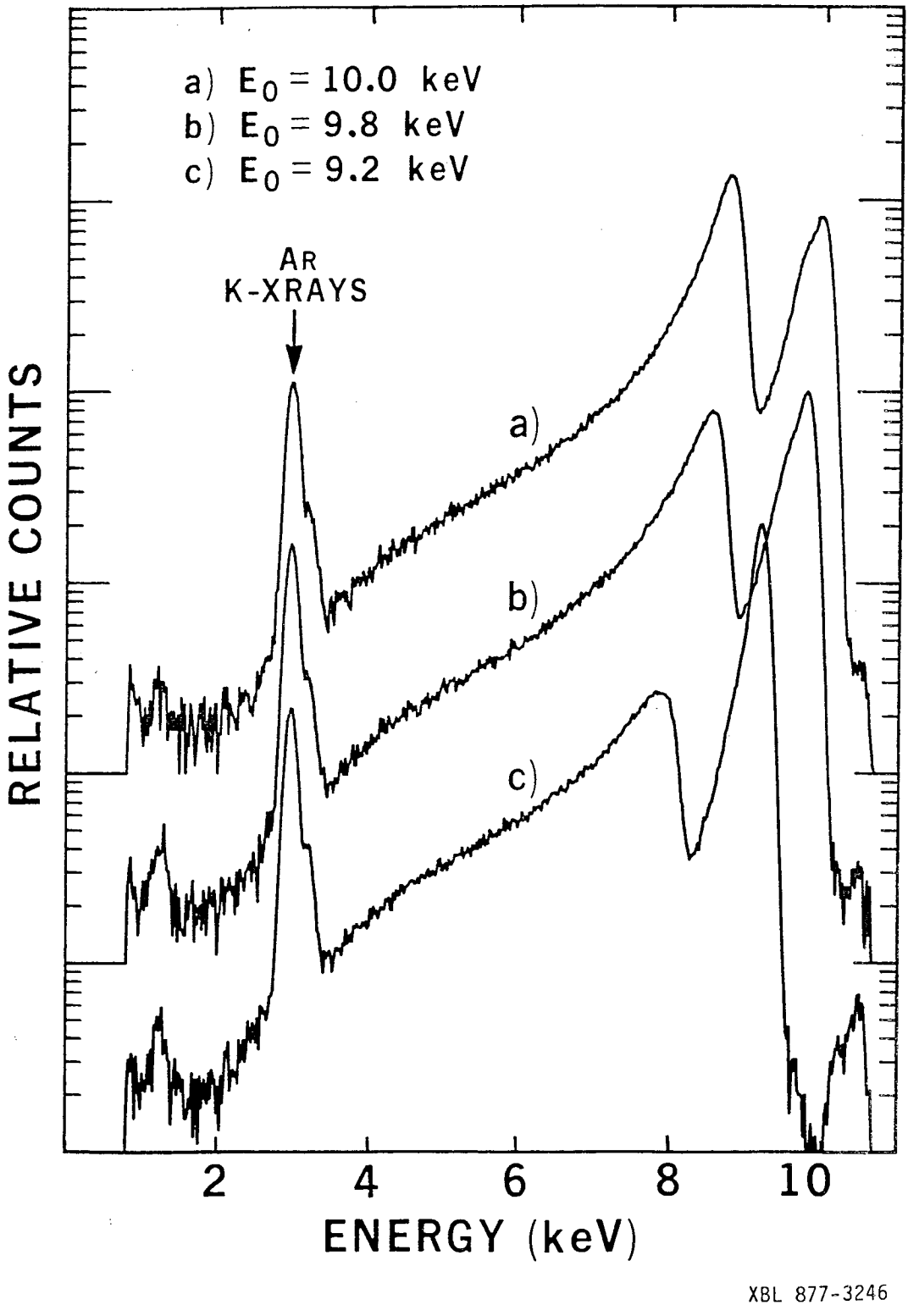

FIG. 5. Scattering spectra obtained from a GaAs sample for three excitation energies near the K-absorption edges of the major constituents. The constant energy interval between the elastic scattering peak and the upper edge of the continuum inelastic peak is indicative of Raman scattering.

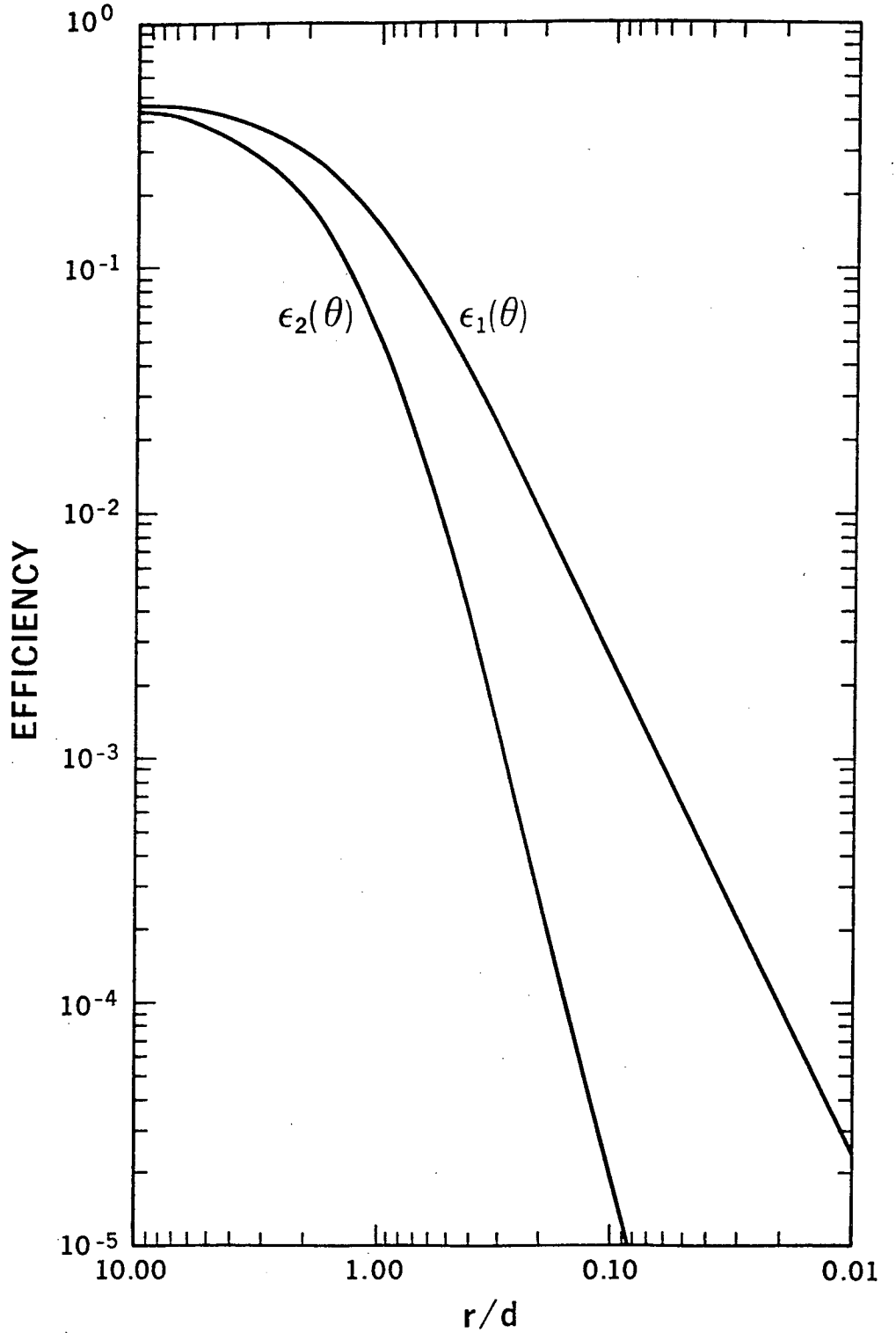

FIG. 6. Efficiency for detection of isotropic, ε_1 (θ), and anisotropic radiation described by Eqn (4), ε_2 (θ).

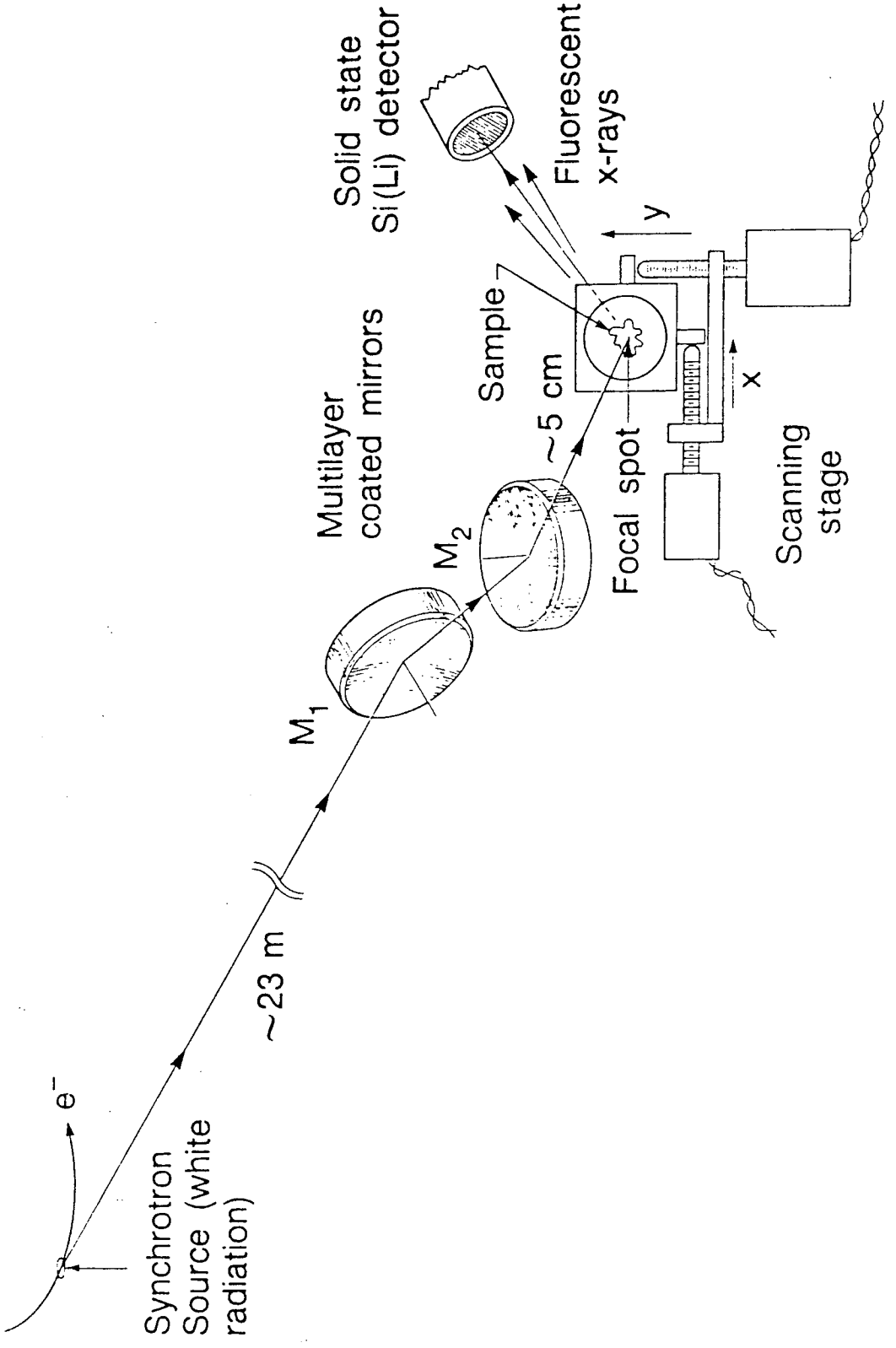

FIG. 7. Schematic of the x-ray microprobe. The tungsten/carbon-coated multilayer mirrors demagnify the source and restrict the bandwidth to 1 keV at 10 keV.

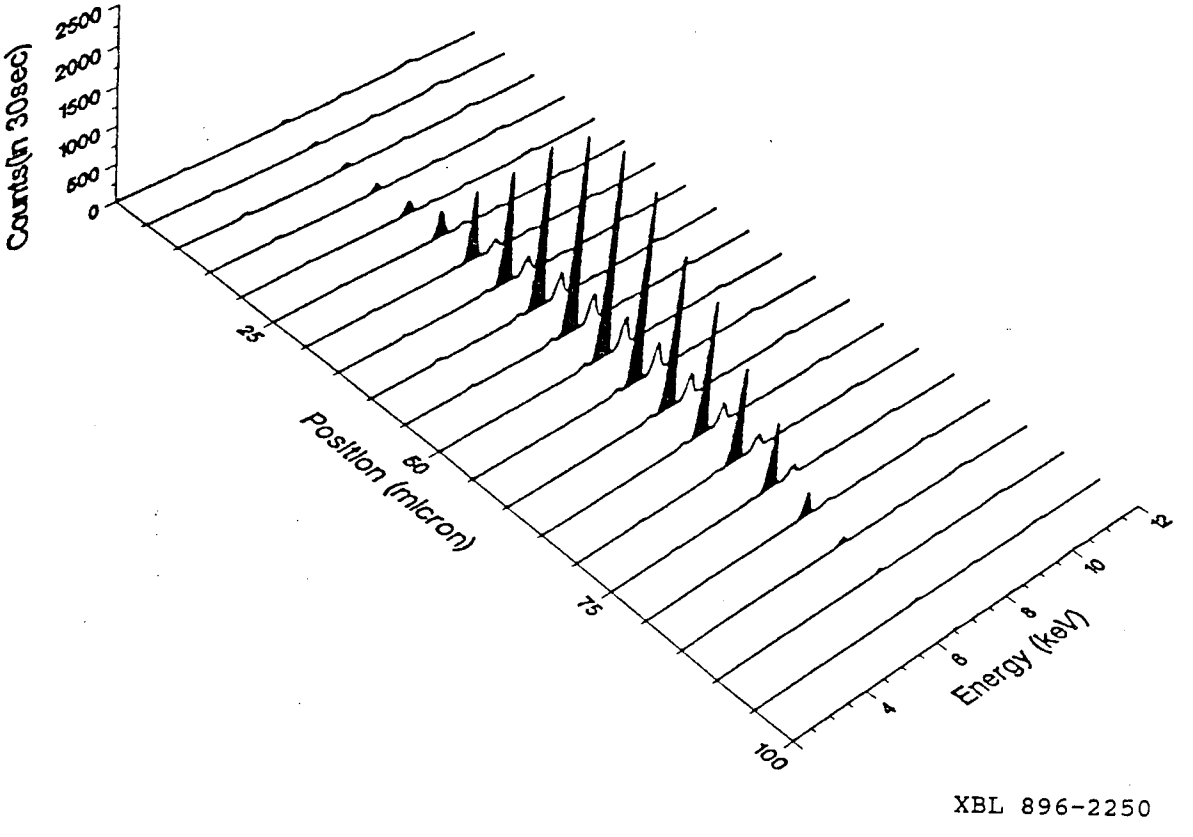

FIG. 8. Scan across a "fox" spot showing the very localized iron concentration. The iron concentration at the peak is 130 $\mu g/cm^2$.

LAWRENCE BERKELEY LABORATORY
TECHNICAL INFORMATION DEPARTMENT
1 CYCLOTRON ROAD
BERKELEY, CALIFORNIA 94720